N. Ardey, F. Mayinger

Aerosol Resuspension by Highly Transient Containment Flow - Insights by Means of Laser Optical Methods

Within the course of a hypothetical core melt accident in a light water reactor, several physical processes lead to the formation of active and non active aerosols. During the accident sequence, a considerable part of the aerosols is deposed within the containment. Transient flow situations during the late phase of an accident (blow-by, H_2-explosions, etc.) can resuspend primarily deposed aerosols to a considerable extent - an effect, which is not yet well understood and not yet taken into account within any containment simulation code. Therefore, an experimental study of the aerosol resuspension in transient flows by means of highly resolving, laser-optical techniques is presented in the present paper.

Resuspension von Aerosolen durch hochtransiente Containment-Strömungen - Einblicke durch Laser-optische Methoden. *Im Verlauf eines hypothetischen Kernschmelzunfalls in einem Leichtwasserreaktor führen verschiedene physikalische Prozesse zur Freisetzung radioaktiver und nicht aktiver Aerosole. Während des Unfallablaufs wird ein beträchtlicher Anteil der Aerosole innerhalb des Containments wieder abgeschieden. Transiente Strömungsvorgänge in der Spätphase derartiger Unfälle (Blow-by, H_2-Abbrand, u.s.w.) können die Resuspension erheblicher Mengen an Aerosolen nach sich ziehen - ein Vorgang, der bis heute weder gut verstanden, noch in derzeitigen Containment-Simulations-Codes berücksichtigt ist. Deshalb wird in diesem Beitrag über eine experimentelle Studie zur Resuspension durch transiente Strömungswellen mit Hilfe hochauflösender, Laser-optischer Verfahren berichtet.*

1 Introduction

The major source of aerosol release during a hypothetical core melt down accident is the formation of finest droplets due to condensation processes in-vessel and in the containment atmosphere. Other mechanisms of aerosol release are fragmentation of partially solidifying core melt during interaction with water, erosion of steel and concrete material in case of a failure of the reactor pressure vessel and the consequent entrainment of molten material into the ex-vessel containment, etc.. The emerging mix of aerosols is therefore a composition of non-soluble aerosols (e.g. UO_2, steel, concrete, …), soluble and hygroscopic parts (e.g. CsOH, CsI, …) and liquid parts (water droplets, …). The corresponding particle size distribution is considered to range from 0.1 to 5 µm, although reliable data are not yet available. Resuspension of deposed aerosols additionally loads the containment venting filters and, can cause a blow-through of the filtering system. If the containment hypothetically fails by overpressure, the aerosols are released to the environment either directly or through several leakages. Hence, the resuspension of aerosols by containment flow effects has to be considered for the behaviour of fission products and the corresponding assessment of accident consequences to the environment.

Up to now, experimental work on aerosol resuspension almost solely treats steady state flow phenomena in tubes and their interaction with the aerosol layer. Resuspension- and deposition-effects are rather difficult to distinguish from the experimental results, since both phenomena are superimposed in most of the known experimental programs. Some of the most important programs are listed in table 1 ([1], [2], [3], [4], [5], [6], [7]). In comparison with steady flow phenomena, transient flow phenomena generally do not have a homogeneous and stable velocity profile. The formation or degradation of turbulent boundary layers and the local flow gradient have strong effects on aerosol resuspension which are not addressed by steady state flow experiments.

Only two experimental programs are known which partially address aerosol resuspension by transient flows. Nelson et al. performed add-on experiments to the FLAME-program with H_2-deflagrations running over an aerosol layer within an explosion tube of 1.8×2.4×30.3 m at Sandia National Laboratories [8]. As a major conclusion it turned out from the FLAME-add-on experiments, that mild deflagrations already yield a resuspended fraction of more than 50% and moderate or violent deflagrations reach even 70%-85%. It is of special interest that no influence of condensed steam could be observed. It was suggested that the H_2O-molecules preferentially absorb the radiation of the H_2-flame and are heated up, thereby, which diminishes their adhesive effect or that they are even fully evaporated by radiation. The second known experiment was performed as an addi-

experimental program	*applied aerosols*	*remarks*
LACE	$NaOH/Al(OH)_3$-compositions, CsOH/MnO-compositions, etc.	Hanford Eng. Lab. 1984-1987, "aerosol retention during a bypass accident", pipe-system (∅=63 mm), [1]
Marviken Experimental Intermediate Program 1985	30% Ag, 60% Cu, 10% Mn	Influence of resuspension on the deposition of particles in pipes, insoluble aerosols, [2]
small scale - Oak Ridge National Lab.	no accident-relevant particles	Pipes, ∅=23.3 mm, determination of the flow velocity on the resuspension rate, [1], [3]
LACE-add-on experiments	insoluble aerosols	Paul Scherrer Institute, emphasis on accident-typical conditions (blow down, ...), determination of erosion- and denudation- effects, [4]
STORM	CsOH, SnO_2, NaOH, $Al(OH)_3$, MnO	JRC Ispra, resuspension rate in pipes at flow velocities of 50-200m/s and temperatures of 100-1100°C in H_20-air- / N_2-air- mixtures, [5], [6], [7]

Tab. 1: Experimental programs on aerosol resuspension (steady flow)

tional scoping test (Mx7) within the scope the VANAM program by Kanzleiter at Battelle I.G. Eschborn in the Battelle Model Containment. It turned out also from these experiments that mild deflagrations already yield considerable high resuspension rates [9], [10], [11]. Due to the integral character of the VANAM- and the FLAME experiments, both programs mainly delivered coarse data about the global aerosol behaviour at a technical scale. Within the three dimensional geometry at large scale, numerous effects are superimposed (scale, multi-compartment geometry, stagnation zones, recirculation zones, shear layers, ...). Hence, a separate analysis of those effects on the resuspension process is almost impossible.

In order to gain a more detailed access to the physical effects, a complementary program on small scale experiments of a fundamental character is required, which enables the application of sophisticated, highly resolving instrumentation (laser-diagnostics, high speed optics, ...). The main goal of the present study, was therefore to determine the main phenomena and effects on the interaction between a transient flow wave and an aerosol layer as a scientific base for the definition of such a program. Appropriate optical diagnostics were developed and qualified for the application to highly transient resuspension processes.

2 Theoretical Aspects

A common formulation of the resuspension process of deposed particles is based on a balance of all forces applied to a particle. The main reference value is the minimum flow velocity, where aerodynamic lift plus viscous drag and adhesion sticking the particle to the boundary surface counterbalance each other. When humidity leads to additional adhesion / cohesion by capillary forces and surface tension, this reference velocity reaches a maximum.

According to Parozzi [12], the resuspension rate Λ of dry particles can be calculated as follows:

$$\Lambda(D_P) = 1.8 \cdot F(D_P)^{0.88} \qquad (1)$$

$F(D_P)$ represents the total sum of every force applied to the particle, which mainly depend on the particle diameter D_P and comprise:

gravity forces $F_G = (4/3)\pi(D_P/2)^3 \rho_P g$

friction and adhesion $F_{A,f} = f \cdot F_G \quad ; \quad f \approx 0.2$

cohesion $F_{A,C} = HD_P \; ; H \approx 4 \cdot 10^{-7} N/m$

aerodynamic drag $F_{R,d} = \tau_0 \pi (D_P/2)^2$

(τ_0 wall shear stress)

aerodynamic burst $F_{R,b} = 21 \rho \nu^2 (D_P U^*/\nu)^3$

with the wall shear

stress velocity $U^* = \sqrt{\tau_0/\rho}$ (2)

The analytical formulation of the components of adhesion (molecular interaction, electro-statical interaction, capillary effects) with the assumption of spherical particles, generally exhibits a linear relationship to the particle diameter [13], [14], [15]. Hence, it is also common to treat adhesion and friction separately. However, attempts of analytically modelling of adhesion normally fail due to the heterogeneous particle shape. Therefore, only semi-empirical models on the total adhesion are available, which strongly depend on the corresponding experimental apparatus. The only available relation taking into account humidity can be found in [16]:

$$F_{Ad} = 0.15 \cdot D_P \cdot [0.5 + 0.0045 \cdot (\%rel.humidity)] \qquad (3)$$

The aerodynamic burst forces predominantly apply to larger particles with a diameter of several µm perpendicular to the boundary surface. They appear due to turbulent fluctuations within the viscous sublayer, when fluid domains faster than the local average are pushed towards the boundary surface and those being slower are driven away from it (cf. fig. 1). These effects preferentially appear during the formation of

turbulent boundary layers in transient flows and propagating flow waves.

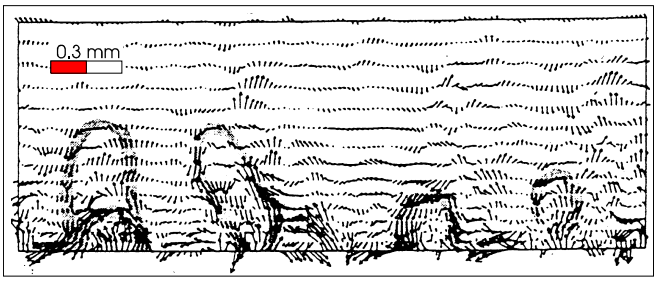

Fig. 1: Snapshot of the flow field within a turbulent, viscous sublayer (simulation) [17]

For transient flow situations, the force balance concept does not fully describe the process of particle removal from the boundary surface. If a constant, horizontal force is applied to a spherical particle within a potential valley, the particle is subjected to a constant displacement. However, when the force changes in time, the whole system starts to oscillate. Exceeding a certain amplitude, respective oscillation energy, the particle overcomes the potential wall and escapes. For resuspension processes the gravity forces have to be supplemented by adhesion. I.e., resuspension by transient flow phenomena can be described by an oscillation approach which partially has been shown by Reeks et al. [18].

Altogether, systematic theoretical and experimental investigations of the several separate phenomena are still at a basic level, since reliable data on the involved forces, aerodynamic effects and the particle-particle interaction are not available, yet [19-26]. A certain part of the removed particles remains within the boundary layer and is deposed again right behind the location of removal. Special attention is paid to the contribution of aerosol resuspension to the total amount of radioactivity to the environment. Therefore, it is necessary also to include particle penetration into the main flow domain for the general consideration of resuspension processes during severe accidents. For the simulation of aerosol transport and aerosol behaviour in the gaseous phase, the particle size distribution of resuspended aerosols is another key parameter.

3 Experiments

3.1 Test facility

To investigate the resuspension of deposed particles by transient flow phenomena (H_2-burn, etc.), a windtunnel has been employed in order to generate flow waves on a high level of reproducibility (cf. fig. 2). The windtunnel is supplied by a pressure reservoir (vessel). Viscosity and density of the fluid are controlled by the initial temperature of the vessel which is equipped with an electric heater. The experiment is started by an abrupt expansion of the vessel content by means of a high speed ball valve and/or a rupture disk.

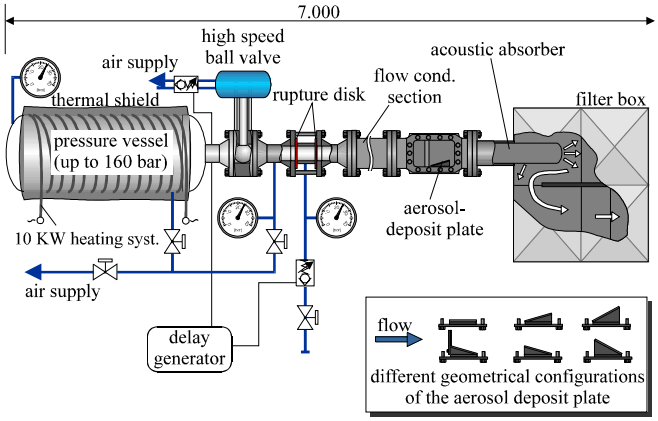

Fig. 2: AeReST facility (Aerosol Resuspension Shock Tube)

The initial pressure, initial temperature and the ball valve end-position determine the duration and intensity of the released flow wave (cf. fig. 3).

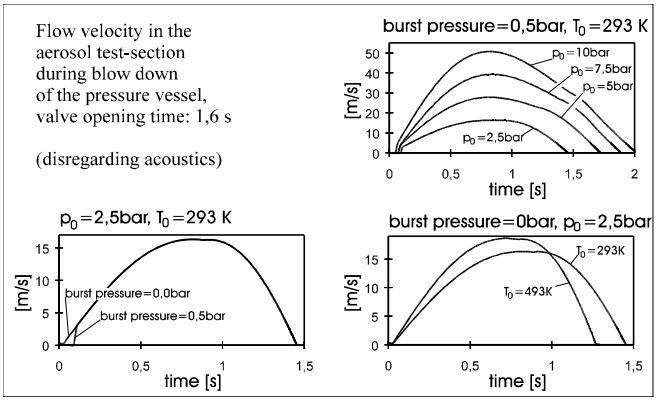

Fig. 3: Blow-down characteristics of the AeReST facility

Within a flow conditioning section the leading shock wave is broken by means of built-ins and the flow is parallelised by honeycombs. Right behind the conditioning section the expansion wave is transmitted to the optically accessible test section with the aerosol deposition plate at the bottom. The different geometric configurations of the aerosol deposition plate which have been tested are shown in fig. 2. In order to suppress acoustic oscillations inside the flow channel, an acoustic absorber is connected to the test section. Finally, the resuspended particles are trapped in a filter box.

In the present study, mainly TiO_2-particles ($D_P \approx 1\mu m$) have been applied which are generated by crystallisation out of a solution by crystallisation seeds. A systematic variation of the aerosol type remains a future task for the ongoing program. The aerosol layer (0.1-5 mg) was deposed on the aerosol deposition plate as a stripe of 10×1 cm^2 by a template within a gravitational settling chamber. By means of a swirl chamber and a pinhole primary particles of TiO_2 were injected to the settling chamber.

3.2 Instrumentation

Beside conventional instrumentation such as fast responding pressure transducers and - thermocouples and a µg-scale for balancing the total mass of the deposit before and after the experiment, the main emphasis has been put on optical diagnostics showing a high time resolution of the resuspension process.

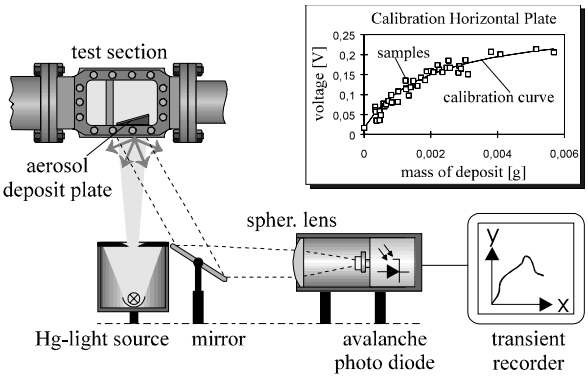

Fig. 4: Light scattering method for the time-resolved detection of the total mass of deposit

To detect the total mass of deposit during resuspension, a light scattering method has been developed (cf. fig. 4). The aerosol layer, deposed on a transparent glass plate, is illuminated by a constant-light source. By means of an avalanche photo diode and a thermally compensated and noise reduced amplifier, the scattered light originating from the deposed particles is detected. The calibration of the technique is a by-product of the fine-scaling before and after the experiment. The sensitivity of the voltage signal on the total mass of deposit is shown by the calibration curve for the horizontal aerosol deposit plate in fig. 4. Due to the influence of the plate geometry and the type of aerosol on the light scattering, calibration is necessary for each aerosol deposit plate and each type of aerosol tested. With an increasing thickness of the aerosol layer, the sensitivity of this method decreases. However, within the required range of a few mg of aerosols, good results have been obtained by the scattering method.

The amount of resuspended particles has been detected locally by means of a laser-extinction method (cf. fig. 5), which takes advantage of the increasing absorption coefficient α with an increasing particle density. Due to the absorption law

$$\Delta U = U_0 \cdot e^{-\alpha \cdot l} \qquad (4)$$

with the difference-amplifier output ΔU, the maximum difference voltage U_0 and the reference length l, and the calibration law for the particle density ρ

$$\alpha = \frac{110 \cdot \rho}{\rho + 3 \cdot 10^{-2}} \qquad (5),$$

the following relation between particle density ρ and the voltage signal ΔU is obtained:

$$\rho = \frac{3 \cdot 10^{-2} \cdot \ln\left(U_0 / \left(U_0 - \Delta U\right)\right)}{110 \cdot l - \ln\left(U_0 / \left(U_0 - \Delta U\right)\right)} \qquad (6).$$

The reference length l corresponds to the length of the beam within the probe volume.

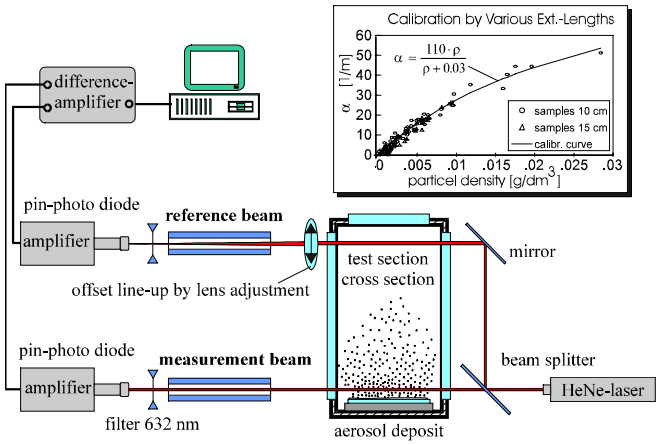

Fig. 5: Laser-extinction method for the detection of the particle density of resuspended aerosols

The extinction method has to be calibrated separately. For that purpose experiments have been carried out with several test chambers of different lengths. The well predefined amount of particles, injected into the test chambers was kept stirred by free convection generated by a heated bottom plate. In transient flows, the laser beam is slightly deflected, when the propagating density front of the flow wave passes the probe volume. In order to compensate the corresponding signal, a reference beam was located exactly at the horizontal location of the measurement beam and at a certain height over the aerosol deposition plate, where no particles from the deposit are to be expected. The difference of both signals is therefore purely dependent on the particle density along the measurement beam.

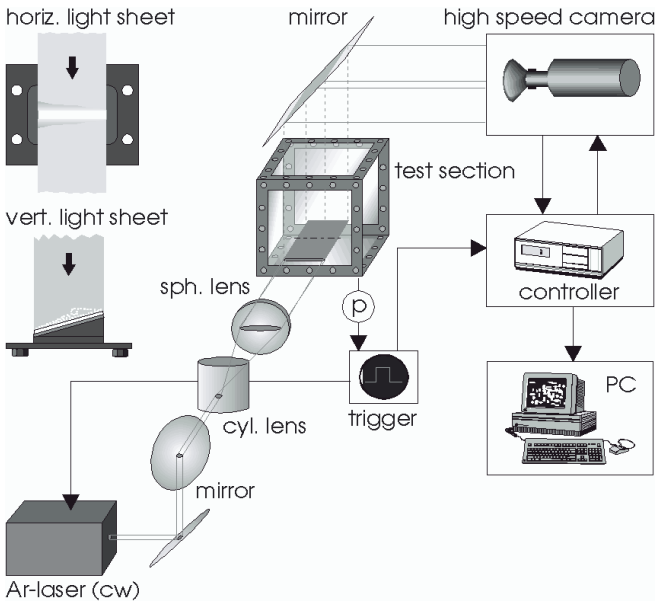

Fig. 6: Set-up for high speed - particle tracking

In order to visualise the mentioned phenomena of particle resuspension, the particle movement has been recorded by high speed particle tracking (cf. fig. 6). The particles have

been illuminated by a laser light sheet and recorded by a high speed ccd-camera (max. 40,000 frames per sec.). Due to the different orientations of the laser light sheet, the particle movement has been measured in both vertical and horizontal planes.

4 Results and Discussion

4.1 Time resolved measurements

A survey on the simultaneously recorded signals from the above mentioned methods is shown in fig. 7. Due to the abrupt burst of the diaphragm, an acoustic wave propagates in front of the main flow wave which can be determined from the pressure- and the corresponding flow history. Because of the acoustic absorber behind the test section, reflected pressure waves are suppressed and the precursor acoustic wave rapidly decays.

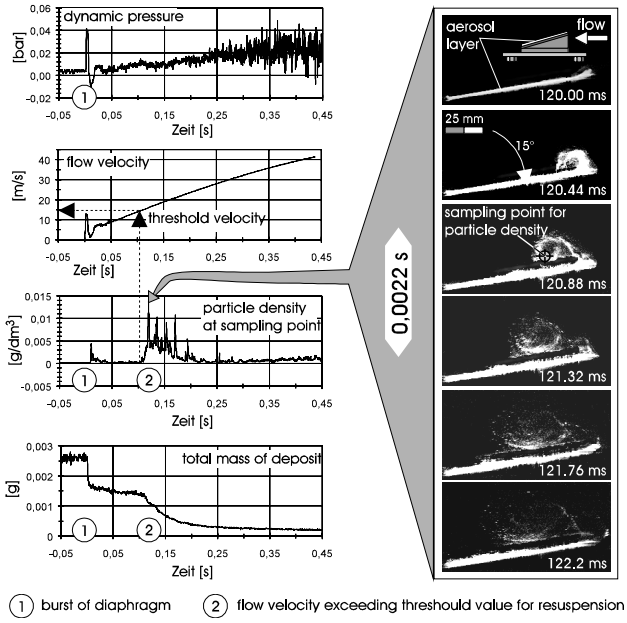

Fig. 7: On-line data of particle resuspension by a passing flow wave (aerosol deposition plate inclined by 195° to the main flow direction, initial vessel pressure 5 bar)

The frame sequence in fig. 7 is a record of the particle removal by a single vortex, which separates at the leading edge of the aerosol deposition plate. The whole sequence (2.2 ms) corresponds to one of the single spikes in the diagram of the particle density. Right upon the aerosol layer a recirculation zone appears, within which the particles first move towards the leading edge of the deposition plate, where they are removed from the plate and driven upward.

Obviously, the resuspension process is almost completed within the very first phase of the flow wave (ca. 0.3-0.6 sec. after the leading pressure wave). During the remaining phase, the resuspension process is just creeping with only few particles removed per second. I.e., in case of a hydrogen burn, the resuspension process is limited to the vicinity of the flame front, where the maximum heat release is to be expected. This effect is suggested to be one reason for the high resuspension rates also observed in a wet atmosphere [8].

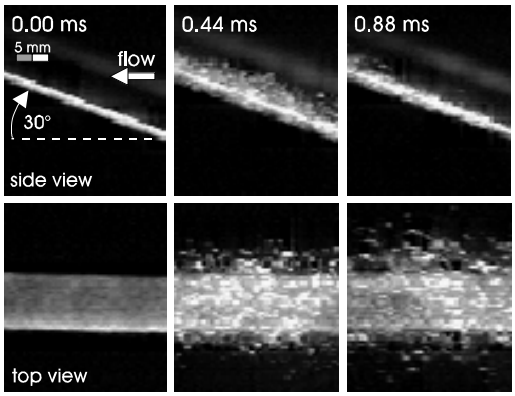

Fig. 8: Particle removal by the leading pressure wave

Generally, two steps of particle resuspension have been observed. During the first step, a layer of particles is lifted by the leading pressure wave and shifted by about 100 mm. This process, commonly being referred to as denudation, is exemplary shown in fig. 8 for the aerosol deposition plate with 30° inclination to the flow. Apparently, the particles roughly penetrate into the main flow and remain within a layer close to the boundary surface. This confirms the observation of Fletscher [27] that the particle penetration by a shock wave propagating along a particle deposit does not exceed a value of about 1-3 mm.

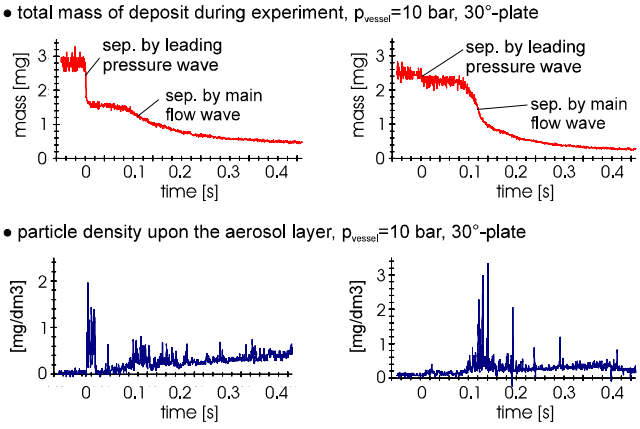

Fig. 9: Resuspension with 10 bar initial vessel pressure and 30°-plate. Left: strong particle removal by leading pressure wave. Right: weak particle removal by leading pressure wave.

The second step of particle removal is some what delayed. This points to a threshold value for the flow velocity under which no particle removal is possible (cf. fog. 8). Depending on the local velocity gradient the threshold velocity w_t varies within the range of:

$$w_t = 8-12\,m/s \quad \text{with} \quad \partial w/\partial t = 43-70\,m/s^2,$$

where the threshold velocity generally increases with a decreasing local velocity gradient. For aerosol deposition plates which are inclined more than 180° to the flow, the threshold velocities appeared to be higher:

$$w_t = 12-17\,m/s.$$

This can be explained by the fact that the aerosol layer is located within a recirculation zone with lower corresponding boundary-flow velocities.

With about 12 m/s, the maximum acoustic flow velocity corresponding to the leading pressure wave is within the range of the threshold velocities (cf. fig. 7). Hence, the particle removal by the leading pressure wave was not observed in any case (cf. fig. 9). With an initial vessel pressure of 2.5 bar the threshold velocity was even not reached by the main flow wave. I.e., the particle resuspension was caused only by the leading pressure wave. If the pressure wave itself did not exceed the threshold velocity, almost no resuspension was observed (cf. fig. 10). All together, considerable data scattering is caused by the leading pressure wave.

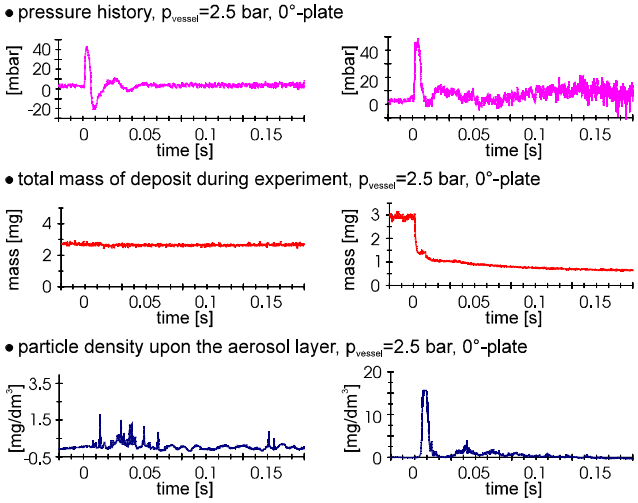

Fig. 10: Particle resuspension with 2.5 bar initial vessel pressure and horizontal plate. Left: almost no particle removal. Right: Particle removal only by the leading pressure wave.

From the plots in fig. 11 it can be derived that the removal of particles by the leading pressure wave has a substantial influence on the resuspension process, thereafter. The very first particle removal leaves a crater-structure with lots of grooves in the original aerosol deposit. Thereby, the effective surface which is exposed to the flow for further particle removal increases. Additionally, the increased roughness of the surface leads to an incitement of flow fluctuations within the viscous sublayer. Hence, the particle removal by the main flow wave is stronger with a pre-damaged deposit by the leading pressure wave (cf. fig. 11).

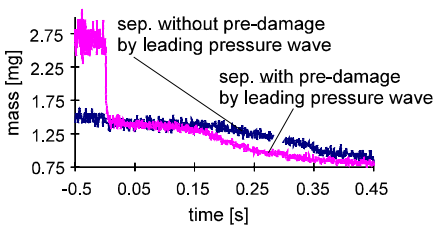

Fig. 11: Total mass of deposit during experiment with 2.5 bar initial vessel pressure and 30°-plate - comparison: with/without pre-damage of the deposit by the leading pressure wave.

Since particle removal by the leading pressure wave was not observed in any case, the particle removal by the main flow wave was also subjected to a considerable data scattering. Therefore, a systematic evaluation of the dependence of the threshold velocity on the local gradient of the flow velocity was not possible. For that purpose it is proposed to perform an experimental series without any burst diaphragm, but at high initial vessel pressures in order to obtain the required high local gradients of the flow velocity.

The influence of the initial vessel pressure with the corresponding flow velocity and its local gradient is shown by an increasing resuspension effect with an increasing vessel pressure as expected (cf. fig. 12).

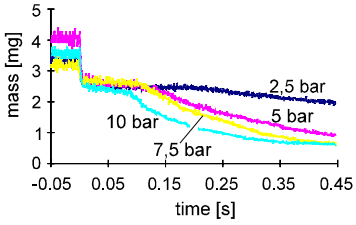

Fig. 12: Total mass of deposit during experiments with various initial vessel pressures, 15°-plate.

Except the particle removal with 2.5 bar, all curves converge to a common saturation value, which is reached after approximately 0.6 s by all removal curves. This has been observed also for the aerosol deposition plates with 195° and 210° inclination to the flow. With 0° and 30° inclination, even the 2.5 bar-curves converge to the same saturation value. Hereby, the aerosol layer is removed until the thickness of the remaining layer reaches a value, where the adhesion between particle and boundary surface dominates the force balance with the aerodynamic lift of the particles. Obviously, the particle/boundary surface adhesion is significantly higher than the particle-particle adhesion, which dominates the resuspension process at the beginning. For TiO_2-particles, it is also higher than the gravity forces. I.e., for most of the considered geometries, the same total amount of removed particles can be taken for dry resuspension, if the maximum flow velocity significantly exceeds the threshold velocity for at least 1s. This total amount (maximum particle removal) mainly depends on the thickness of the aerosol layer and the type of aerosols.

However, for transient flow phenomena corresponding to mild deflagrations (conditions of 2.5 bar initial vessel pressure) and flow phenomena with a duration less than 1s, the short term behaviour has a strong impact on the total particle removal. Hence, for those conditions, the resuspension process is to be modelled as a function of time. Generally, the removal curves show an exponential behaviour, which also has been observed by Braaten et al. [19]:

$$\text{remaining part} = A \cdot e^{-Bt} \qquad (7)$$

With regard to the saturation value, eq. 7 has to be supplemented by an additional constant:

$$\text{remaining part} = S + (M - S) \cdot e^{-Bt} \qquad (8)$$

with the saturation value *S*, the total mass of deposit *M* and the decay value *B*. *S* and *B* are functions of the flow velocity and its local gradient, the local turbulence intensity, the boundary material and the type of aerosol. With presently available containment simulation tools local values of turbulence and flow gradients are commonly not accessed. This leads to the necessity of a classification of representative geometries with a corresponding parameterisation of the considered flow situations. However, such a parameterisation is strongly subjected to scaling effects.

4.2 Total resuspended fraction

The described separate phenomena of dry resuspension by transient flow waves show the expected effects on the total particle removal, which was detected by fine-scaling right before and after the experiment. For a comparison of the experimental results a resuspended fraction Λ was defined:

$$\Lambda(\%) = \frac{m_v - m_n}{m_v} \cdot 100 \qquad (9)$$

with the total mass of deposit before the experiment m_v and after the experiment m_n. The total resuspended fraction, again shows a high data scattering due to the scattered resuspension by the leading pressure wave, which should be circumvented by experiments without any burst diaphragm and correspondingly increased initial vessel pressures for future experiments.

In fig. 13 a comparison of the experiments with the horizontal aerosol deposition plate with TiO_2 and Ag at ambient temperature and with TiO_2 at an elevated temperature is shown. Generally, the total resuspended fraction shows the same behaviour for all pressure values, which confirms the observation of a saturation value from the online measurements of the total mass of deposit.

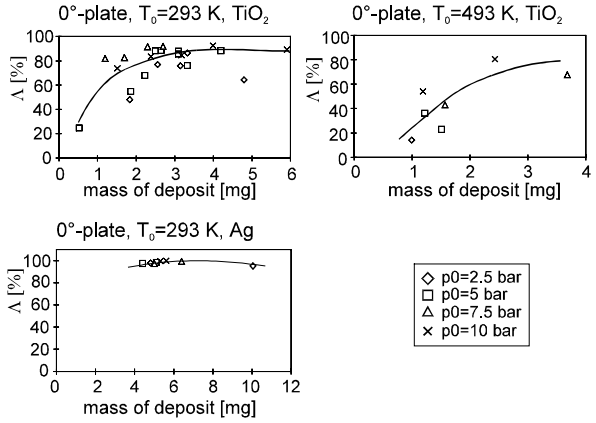

Fig. 13: Total resuspended fraction, experiments with horizontal aerosol deposition plate.

The resuspended fraction increases with an increasing thickness of the deposit layer, as expected, since the particle-particle adhesion is much lower than the particle-boundary surface adhesion. In contrast to the experiments with TiO_2, the experiments with Ag, throughout, show an almost complete removal of the deposed particles. The main reason for that behaviour is the larger particle diameter of 10-100 µm in contrast to 0.3-1.5 µm of the TiO_2-particles and the corresponding low boundary shear stress which is necessary for particle removal. Additionally, the particle removal is favoured by the strong polydisperse character of the employed Ag-powder.

Originally, it was intended to demonstrate the influence of the increasing kinematic viscosity ν by the experiments at elevated fluid-temperature. With an initial vessel temperature of 220°C, a maximum fluid temperature of about 70°C could be achieved in the test section, due to the expansion of the flow and heat losses to the channel walls. Due to the decreasing density ρ with increasing temperature, the dynamic viscosity η=ρν, which is the relevant parameter for the wall shear stress, does not significantly change with increasing temperature. However, the specific momentum flux ρw^2, which decreases with increasing temperature, appeared to be the dominating parameter. I.e., the total resuspended fraction is lower with elevated fluid-temperatures (cf. fig. 13).

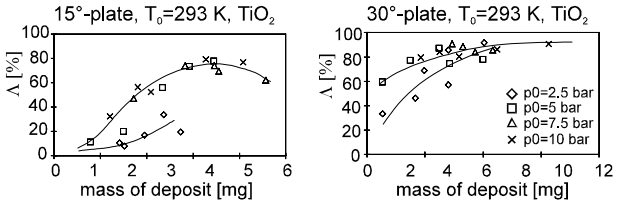

Fig. 14: Total resuspended fraction with aerosol deposition plates, inclined by 15° and 30° to the main flow.

If the aerosol layer is inclined to the main flow, the total resuspended fractions get spreaded by the initial vessel pressure (cf. fig. 14). The resuspended fractions, hereby, are significantly lower than the resuspended fractions at higher initial vessel pressures. The data spread between 2.5 bar and the higher pressures, as well as the dependence of the resuspended fraction on the initial mass of deposit most strongly appeared with the 15°-aerosol deposition plate. Obviously, the turbulent fluctuations are reduced by the 15°-plate. Similar to a slightly convergent flow channel, the vorticity is reduced by a bundling and alignment of the streamlines. However, with a further increase of the angle of incident, the typical pair of vortex is formed within the stagnation zone and the turbulence intensity increases again. Due to the corresponding increase of the resuspended fraction, the 30°-plate again shows similar values to the resuspended fractions with the horizontal plate.

For the aerosol deposition plates with 195°- and 210° inclination to the main flow, significantly higher resuspended fractions were expected, due to the flow separation at the leading edge of the aerosol deposition plate and the resulting, strong fluctuations within the recirculation zone. Nevertheless, the increased data scattering - especially with 2.5 bar initial vessel pressure - turned out as the main difference to the experiments with angles of incident below 90° (cf. fig. 15). Obviously, the influence of macroscopic vorticity on the particle removal is much less pronounced than the effect of the micro-vorticity within the viscous sublayer. The

micro-vorticity within the viscous sublayer almost solely depends on the convective velocity gradient within the boundary layer and the wall roughness and is hardly affected by the macro-vorticity.

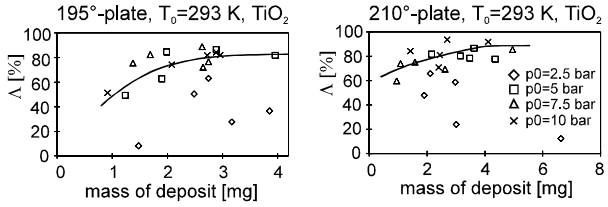

Fig. 15: Total resuspended fraction with aerosol deposition plates of 195°- and 210° inclination to the flow.

The macroscopic vorticity mainly determines the penetration of removed particles in the main flow field by its characteristic length scales which, in turn, are determined by the local geometry (cf. fig. 7). I.e., the resuspended fraction is not the only key-parameter to be considered for the overall aerosol balance. In contrast to the partially obstructed flow situation, the vorticity of an unobstructed pipe flow does not drive the particles more than about 1-3 mm away from the boundary surface [27], which was confirmed by the observations within the scope of this study. This points to the suggestion, that a considerable part of removed particles is deposed again right in the vicinity of the location of removal. The observed track of particles just behind the aerosol deposition plate is another indication for that suggestion. Future experiments, therefore, have to address re-deposition behind the resuspension area as well as particle penetration into the main flow region.

The experimental results with the 90°-deposition plate exhibit a completely scattered data field without any structure (cf. fig. 16).

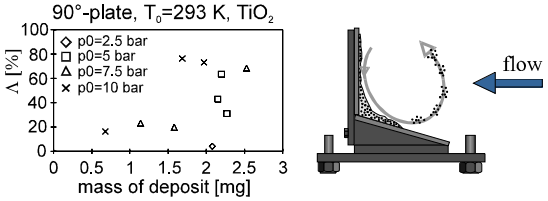

Fig. 16: Total resuspended fraction with vertical aerosol deposition plate.

It could be observed from the high speed particle tracking records, that a large scale vortex is formed in front of the plate, which slowly drives the particles downward along the plate surface. At the bottom in front of the vertical plate, the particles form a deposit which is similar to snow-drifts in front of slopes. From there, particles are removed again by the large scale vortex, driven upward and deposed again at the aerosol deposit plate (cf. fig. 16). Due to the whole flow situation, the data scattering is not surprising.

5 Conclusions

Due to the complexity, non-linearity and stochastic character of the physical processes of aerosol resuspension, the concerned effects are difficult to determine experimentally as well as theoretically and just hardly understood, at the time being. Attempts of analytical modelling base on strong idealistic assumptions and rely on an incomplete data base. Experiments at a technical scale, generally, involve problems of the separation of different phenomena, due to their superimposition. Furthermore, transient flow situations can hardly be kept reproducible at a larger (3D-) scale.

Therefore, lab-scale experiments with reproducible flow waves have been performed, in order to identify the key-parameters of aerosol resuspension and to demonstrate and to qualify appropriate measuring techniques to access the concerned physical effects beside the already improved balancing methods. Three optical methods have been employed:

- laser-extinction method for the time resolved detection of the particle density within the flow,
- scattering method for the time resolved measurement of the total mass of deposit and
- high speed particle tracking for the visualisation of particle motion.

Simultaneous application of these complementary methods, together with balancing techniques delivers comprehensive information on the whole process.

As an important key parameter a threshold velocity for particle removal has been determined from the experiments. In transient flows, the threshold velocity additionally depends on the local velocity gradient. If the threshold velocity is significantly exceeded by the main flow, a maximum resuspended fraction is reached within a rather short period of time (<1 s) only depending on the aerosol layer itself (type of aerosol, thickness of the layer, material of the boundary surface). For flow phenomena with a duration less than 1 s or with a maximum flow velocity not significantly higher than the threshold velocity, the temporal characteristics of the resuspension process has to be taken into account, which, generally, exhibits an exponential behaviour.

Due to the scattering of the experimental data, a systematic and quantitative determination of the dependency of the threshold velocity on the local velocity gradient requires a huge number of experiments to ensure statistical reliability, which is not provided to a sufficient extent within the scope of this study. Future experiments should be performed without any burst diaphragm, but with higher vessel pressures in order to reduce the data scattering and to cover the complete range of local velocity gradients.

For the contribution of aerosol resuspension to the total amount of aerosols within the containment atmosphere, the particle penetration in the main flow zone as well as the corresponding size distribution after separation from the boundary surface has to be treated separately as further key-parameter. Furthermore, future experiments have to consider wet aerosol deposits as well as a wet flow, which either has not been addressed within the scope of this study.

6 Nomenclature

Λ	resuspended fraction	F_{Ad}	adhesion
ρ	density	F_G	gravity force minus

			aerostat. buoyancy
ν	kinematic viscosity	$F_{R,b}$	aerodynamic burst
η	dynamic viscosity	l	reference length
α	absorption coeff.	M	init. mass of deposit
τ_0	wall shear stress	m_n	mass of deposit after experiment
ΔU	voltage difference	m_v	init. mass of deposit
A	constant	S	saturation value
B	decay constant	U^*	wall shear stress velocity
D_P	particle diameter	U_0	max. voltage
$F_{A,C}$	cohesion	w_t	threshold velocity
$F_{A,f}$	adhesion+friction		

7 Acknowledgement

It is gratefully acknowledged, that the work presented in this paper has been supported by the German Ministry of Education, Science, Research and Technology BMBF.

8 References

1 *Rahn F.J., Sher R., Vogel R.C.:* Summary of the LWR Aerosol Containment Experiments (LACE) Program, proc. of the IAEA/NEA International Symposium on Severe Accidents in Nuclear Power Plants, Sorrento, Italy, 1988

2 *Stroem L.:* Resuspension of Dust Deposits in Pipes, Studsvik - The Marviken Project, Report MXIP-11, 1986

3 *Wright A.L.:* Series-2 Aerosol Resuspension Test, Data Summary Report, Oak Ridge National Lab., Draft Report NRC FIN No. B0488

4 *Fromentin A.:* Particle Resuspension from a Multy-Layer Deposit by Turbulent Flow, Paul Scherrer Institute, report no. 38, Wuerenlingen, 1989

5 *Eusebi M., Parozzi F., Valisi M., Capitao J. A., De Santi G. F.:* Preparatory Calculations for a New Experimental Program on Dry Aerosol Resuspension Mechanisms (STORM Project), proc. of European Aerosol Conference, Oxford, UK, Sept. 1992

6 *Valesi M., De Santi G. F.:* Proposals for International Benchmarks on Aerosol Physics, international report, Commission of the European Communities, Institute for Safety Technology, JRC Ispra, Italy, 1993

7 *Reyes A. de los, De Santi G. F., Capitao J. A., Alonso A.:* Computer Code Calculations on Aerosol Deposition and Resuspension in the STORM Facility, proc. of the XX. Reunión Anual de la Sociedad Nuclear Española, Cordoba, Oct. 1994

8 *Nelson L. S., Guay K. P.:* Experiments Related to the Resuspension of Aerosols During Hydrogen Burns, SAND86-0867C, 1986

9 *Kanzleiter T.:* VANAM-Mehrraum-Aerosolabbau-Versuch M4 mit Mischaerosol (lösliches und unlösliches Material) und Resuspension durch einen Wasserstoffbrand, Technischer Fachbericht zum BMFT-Vorhaben Nr. 1500 803, 1993

10 *Kanzleiter T.:* VANAM-Mehrraum-Aerosolabbauversuch M2 mit unlöslichem Aerosolmaterial, Technischer Fachbericht zum BMFT-Vorhaben Nr. 1500 803, 1993

11 *Kanzleiter T.:* VANAM-Mehrraum-Aerosolabbauversuch M3 mit löslichem Aerosolmaterial, Technischer Fachbericht zum BMFT-Vorhaben Nr. 1500 803, 1993

12 *Parozzi F.:* Development of Computer Models on the Chemical and Physical Behaviour of Fission Products and Aerosols in the Primary Coolant System of a LWR During a Severe Accident, Part II: FP and Aerosol Transport, ENEL/DSR/CRTN Report N6/91/03/MI, Work performed under the CEC-SCA Contract no. 3558-88-12 EL ISP I.

13 *Ranade M.B.:* Adhesion and Removal of Fine Particles on Surfaces, Aerosol Science and Technology 7, pp. 161-176, 1987

14 *Krupp, H.:* Particle Adhesion, Theory and Experiment, Advan. Colloid Interface Sci., Vol. 1, pp. 113-239, 1967

15 *Corino E.R., Brodkey R. S.:* A Visual Investigation of the Wall Region in Turbulent Flow, J. Fluid Mech. Vol. 37, No.1, pp. 1-30, 1969

16 *Hinds W.C.:* Aerosol Technology, John Wiley & Sons, 1982

17 *Tritton D.J.:* Physical Fluid Dynamics, second ed., pp. 348, Oxford Science Publications, Clarendon Press, Oxford, 1988

18 *Reeks M.W., Reed J., Hall D.:* On the Resuspension of Small Particles in a Turbulent Flow, J. Phys. D., Appl. Phys., Vol. 21, pp. 574-589, 1988

19 *Fairchild C. I., Tillery M.I.:* Wind Tunnel Measurements of the Resuspension of Ideal Particles Atmospheric Environment, Vol. 16, No. 2, pp. 229-238, 1981

20 *Braaten D.A., Paw K.T., Shaw R.H.:* Particle Resuspension in a Turbulent Boundary Layer-Observed and Modelled, J. Aerosol Sci., Vol. 21, No. 5, pp. 613-628, 1990

21 *Jurcik B.,Wang Hwa-Chi:* The Modelling of Particle Resuspension in Turbulent Flow, J. Aerosol Sci. Vol.22, pp. 149-152, 1991

22 *Wu Yee-Lin, Davidson C.I., Armisttead G.R.:* Controlled Wind Tunnel Experiments for Particle Bounce off and Resuspension, Aerosol Science and Technology Vol.17, pp. 245-262, 1992

23 *Nicholson K.W.:* Wind Tunnel Experiments on the Resuspension of Particulate Material, Atmospheric Environment, Vol. 27A, pp. 181-188, 1993

24 *Soltani M., Ahamadi G.:* On Particle Adhesion and Removal Mechanism in Turbulent Flows, J. Adhesion Sci. Vol. 8, No. 7, pp. 763-785, 1994

25 *Cherukat P., McLaughlin J.B., Graham A.L.:* The Inertial on a Rigid Sphere Translating in a Linear Shear Flow Field, Int. J. Multiphase Flow, Vol. 20, No.2 , pp. 339-353, 1994

26 *Rampall I. , Leighton D.T.:* Influence of Shear-Induced Migration on Turbulent Resuspension Int. J. Multiphase Flow Vol. 20, No. 3, pp. 631-650, 1994

27 *Fletscher B.:* The Interaction of a Shock Wave with a Dust Deposit, J. Phys. D, Vol.9, 1976, pp. 197-202

The authors of this contribution

Dipl.-Ing. Nikolai Ardey,
Lehrstuhl A für Thermodynamik,
Technische Universität München, Germany
Prof. Dr.-Ing. Dr.-Ing. E.h. Franz Mayinger,
Lehrstuhl A für Thermodynamik,
Technische Universität München, Germany